Int J Legal Med (2000) 113 : 221–228

ORIGINAL ARTICLE

Toshiro Kita · Toshiko Tanaka · Noriyuki Tanaka
Yoshimasa Kinoshita

The role of tumor necrosis factor-α in diffuse axonal injury following fluid-percussive brain injury in rats

Received: 27 April 1999 / Received in revised form: 26 July 1999

Abstract The immunolocalization of tumor necrosis factor-α (TNFα) after diffuse axonal injury (DAI) is demonstrated using a midline fluid percussion rat model (moderate brain injury of 1000 mm Hg was generated) and the effects of TNFα on the axolemmal permeability using horseradish peroxidase as a tracer. In addition, the accumulation of β-amyloid precursor protein (β-APP) was investigated, which has recently been shown to be a reliable marker for the diagnosis of DAI in cases with fatal head injury. TNFα levels in brain tissues from the impact site and the cortex including the corpus callosum, gradually increased during the first 1 h, rose to a maximal elevation at 3 h, gradually decreased at 6 h and decreased further at 24 h. Horseradish peroxidase (HRP) tracer experiments revealed that primary axonal damage appeared as early as 15 min after impact but rapidly recovered and that 1 h after impact, secondary axonal damage occurred in the corpus callosum and the brain stem. By immunoelectron microscopy it was seen that β-APP accumulated in the axon from 1 h after impact demonstrating that there was functional axonal damage. TNFα reactions were detected in the lysosomes of microglia 30 min after impact and 1 h after impact these reactions were mainly detected in the glial cells (such as microglia, astrocytes and oligodendrocytes) in the corpus callosum and the brain stem. It is generally accepted that TNFα directly induces primary demyelination and oligodendrocyte apoptosis. Therefore, TNFα conveyed from the microglial cells is one cofactor contributing to the formation of the delayed axonal damage observed at these sites. The present study suggests that TNFα conveyed from the glial cells may contribute to the pathogenic mechanism of DAI formation following fluid percussive brain injury.

Key words Traumatic head injury · Diffuse axonal injury · Tumor necrosis factor-α · β-Amyloid precursor protein · Fluid percussion device · Glial cell

T. Kita (✉) · T. Tanaka · N. Tanaka
Department of Forensic Medicine, School of Medicine,
University of Occupational and Environmental Health,
Yahata Nishiku, Kitakyushu 807, Japan
e-mail: kita@med.uoeh-u.ac.jp

Y. Kinoshita
Department of Neurosurgery, School of Medicine,
University of Occupational and Environmental Health,
Yahata Nishiku, Kitakyushu 807, Japan

Introduction

Axonal damage is a frequent finding after traumatic brain injury and the diagnosis of diffuse axonal injury (DAI), which is associated with high mortality and morbidity rates, is of considerable importance in forensic medicine (Geddes 1997). Maxwell et al.(1997) summarized that in human DAI the majority of axons do not undergo immediate disruption at the time of injury (primary axotomy), but rather are exposed to non-disruptive axonal injury leading, after several hours, to disruption (secondary axotomy). Previous reports have suggested that one of the earliest sequelae to non-disruptive axonal injury is the occurrence of axonal swelling i.e. focal enlargements of the axonal diameter and posited to precede secondary axotomy (Povlishock 1992; Maxwell et al. 1997). Pettus et al.(1994) and Pettus and Povlishock (1996) showed that this secondary axotomy is associated with direct perturbation of the axolemma reflected in its altered permeability. In this respect, there are few studies dealing with altered axolemmal permeability and the mechanism has not been fully elucidated. Recent reports have suggested that tumor necrosis factor-α (TNFα) induces primary demyelination and oligodendrocyte apoptosis (Previtali et al. 1997; Akassoglou et al. 1998; Ladiwala et al. 1998) and our previous report showed that TNFα conveyed from various glial cells is an important factor contributing to the formation of percussive brain edema after moderate brain injury (Kita et al. 1997). Therefore, in this paper we show the immunolocalization of TNFα after traumatic brain injury by fluid percussion and the effects of TNFα on the axolemmal permeability using horseradish peroxidase as a

tracer. In addition, we investigated the accumulation of β-amyloid precursor protein (β-APP), which has recently been shown to be a reliable marker for the diagnosis of DAI in cases with a short survival period (Gentleman et al. 1995; Geddes et al. 1997; Bramlett et al. 1997; Yam et al. 1997; Ogata and Tsuganezawa 1999) and estimated the time when functional damage of axons occurred after percussive brain injury. These experimental data can support the practical diagnosis of DAI in the field of forensic medicine.

Materials and methods

Male Wistar rats (Seiwa Experimental Animal, Ooita, Japan: $n = 83$) weighing 300–350 g were used. All animal experiments were performed in accordance with the Committee for experiments with animals at the School of Medicine, University of Occupational and Environmental Health, and performed along the guidelines of the Committee.

Surgical procedure

Recently, reports have shown that midline fluid percussion (MFP) injury in a rat model produced DAI in contrast to the lateral fluid percussion injury rat model (Yamaki et al. 1994; Iwamoto et al. 1997). Therefore, we used the surgical procedure for MFP injury in the rat model. Animals were surgically prepared under sodium pentobarbital anesthesia (60 mg/kg intraperitoneally) by making a 7-mm diameter burr hole in the skull and the dura was exposed 4 mm in diameter over the superior sagittal sinus. A polyethylene tube filled with isotonic saline was placed against the intact dura, fixed securely to the skull with dental acrylic cement and then connected to a fluid percussion device. The device used to produce experimental brain injury was a modified fluid percussion device produced by the department of neurological surgery of Chiba University (Ozawa et al. 1991). The animals were then subjected to an impact pressure of 1000 mm Hg for 20 ms. The device was removed and the skull hole was closed with dental acrylic cement. Normal body temperature was maintained with a hot plate. In sham-operated controls, all surgical steps were conducted, but the rats were not traumatized.

TNF-α assay

For the brain TNF-α assay 25 rats were utilized. The impact cortex site, including the corpus callosum, was obtained at 0 h (pre-impact), 1 h, 3 h, 6 h and 24 h after impact. The tissues were placed in 10 ml/g of homogenization buffer (PBS, pH7.4 containing 1 mM phenylmethylsulfonyl fluoride, 1 mM EP475, 0.1 μg/ml bestatin and 0.02% NaN_3), homogenized using a polytron AG (model PT-MR3000; Kinematica Instruments, Lucerne, Switzerland) and extracted by sonication at 30 W, 120 pulses and 30% duty (model W357, Heat Systems-Ultrasonics, New York) as described in the method of (Matsukawa et al. 1997). We measured the protein concentration of TNF-α in brain extracts using a rat TNF-α ELISA kit (Genzyme, Cambridge, Mass.) according to the method of Matsukawa et al. (1994) where the detection limit of the assay was 1 ng/g tissue. Data were expressed as mean ± SE for five rats. A non-paired t-test was used to determine significance by the Welch t-test and was accepted if $p < 0.05$.

Magnetic resonance analysis

The rats ($n = 3$) utilized for magnetic resonance (MR) analyses were anesthetized intraperitoneally with sodium pentobarbital (60 mg/kg body weight) and analyzed with T2-weighted MR imaging, which was performed using a 4.7 Tesla MR system with a 400-nm horizontal bore and a proton frequency of 200.0 MHz (SIS 200/400; Spectroscopy Imaging System, Fremont, Calif.) before and 24 h after impact. The head of the animal was placed prone in a slotted tube resonator and spin-echo MR images were obtained in orthogonal planes to confirm the desired positioning (acquisition parameters for T2-weighted images: TR = 2500 ms; TE = 80 ms; 256 × 192 matrix; field of view = 40 × 40 mm; 1 excitation, and 11 2-mm coronal slices with 0 mm center-to-center spacing).

Tracer experiment

The tracer experiment was assessed before impact and 15 min, 30 min, 1 h, 3 h and 6 h after impact. The rats ($n = 18$) were pretreated with diphenhydramine hydrochloride (0.5 mg/100 g, intraperitoneal injection) to prevent histamine release and 50 mg/kg horseradish peroxidase (HRP; type VI peroxidase; Sigma, St. Louis, Mo.) was slowly reinfused into the cisterna magna according to the method of Povlishock et al. (1997). At 15 min after the HRP injection the animals were perfused with a solution of sterile saline, followed by a mixture of 4% paraformaldehyde and 0.5% glutaraldehyde in 0.1 M PBS, infused from the left ventricle. The brain was removed and dissected for the electron microscopic visualization of HRP. The strategy used to select specimens for electron microscopy was to rely on the edema as a visual guide of the MR imaging. Then we selected the impact cortex site including the corpus callosum and the brain stem. The specimens were cut into approximately 30–40 μm sections on a microslicer (Dosaka EM, Osaka, Japan) and inserted into a sample mesh pack (Shiraimatsu, Osaka, Japan). Sections were then treated with a solution of 3,3′-diaminobenzidine tetrahydrochloride (DAB) in 0.05 M Tris buffer containing 0.05% H_2O_2 for 10 min at room temperature, thoroughly washed in 0.05 M Tris buffer, post-fixed in 1% osmium tetroxide in 0.1 M PBS for 1 h at 4 °C, dehydrated in an ascending ethyl alcohol series, embedded in Quetol 812 on glass slides and examined in a JEM 1200 EX electron microscope.

Electron microscopy

For transmission electron microscopy, the experiment was assessed before and 15 min, 30 min, 1 h, 3 h, 6 h, 24 h and 48 h after impact and a total of 16 animals were perfused with a solution of sterile saline (37 °C) and then with a Karnovsky solution at 4 °C from the inferior vena cava. The brain was isolated and tissues were taken from the impact cortex site including the corpus callosum and the brain stem, cut into 2-mm-thick slices and post-fixed in 2% osmium tetroxide in 0.1 M PBS at 4 °C for 1 h. Specimens were dehydrated in an ascending ethyl alcohol series and embedded in Quetol 812. Ultrathin sections were stained with uranyl acetate and lead citrate and examined under a JEM 1200 EX electron microscope.

Immunocytochemistry

Antibodies. Polyclonal rabbit anti-mouse TNF-α antibody (Genzyme Corporation, Cambridge, Mass.) diluted to 1 : 100 in 0.1 M PBS was used. This antibody has demonstrated cross-reactivity with rat TNF-α (Merrick et al. 1992).

Monoclonal mouse anti-β-APP antibody (Zymed Laboratories, USA) diluted to 1 : 100 in 0.1 M PBS was used.

Immunostaining procedures. The TNF-α immunoelectron microscopic experiment was assessed before impact and 15 min, 30 min, 1 h, 3 h, 6 h and 24 h after impact using the streptavidin-biotin technique. The immunoelectron microscopic experiment with β-APP was assessed before impact and 15 min, 30 min, 1 h, 3 h and 6 h after impact using the streptavidin-biotin technique. A total of 21 animals were perfused with 0.1 M PBS from the left ventricle and then with a mixture of 4% paraformaldehyde and 0.5% glutaraldehyde in 0.1 M PBS. The brain was removed and dis-

sected into two parts, the impact site including the corpus callosum and the brain stem. The specimens were cut into approximately 2-mm-thick slices and post-fixed in the same fixative for 1 h. Sections approximately 30–40 μm in thickness were made on a microslicer and inserted into the sample mesh pack. Endogenous peroxidase activity was blocked by incubation in a periodic acid solution (Histofine, Code 415021, Nichirei, Tokyo, Japan) for 45 s and endogenous avidin and biotin activities were blocked by the endogenous avidin/biotin blocking kit (Histofine, Code 415081, Nichirei, Tokyo, Japan). After treatment with normal goat serum at room temperature, sections were incubated overnight with the primary antibody at 4 °C. Sections were also incubated with a biotinylated secondary antibody (TNF-α: goat anti-rabbit IgG, Kirkegaard & Perry Laboratories, Gaithersburg, USA; β-APP: goat anti-mouse IgG F(ab')2, EY Laboratories, Calif.) diluted to 1 : 200 with 0.05 M Tris buffer for 1 h at 37 °C and then with a streptavidin-peroxidase complex (Histofine SAB-PO kits, Nichirei, Tokyo, Japan) diluted to 1 : 600 with 0.05 M Tris buffer for 1 h at 37 °C. After incubation, the sections were treated with DAB in 0.05 M Tris buffer containing 0.05% H_2O_2 at pH 7.6 for 10 min at room temperature, washed thoroughly in 0.05 M Tris buffer, post-fixed in 1% osmium tetroxide for 1 h at 4 °C, dehydrated in an ascending ethyl alcohol series, embedded in Quetol 812 and examined under an electron microscope. Controls for each immunostaining were carried out by substituting tris buffer or normal serum for the primary antibodies.

Results

Of the 94 MFP model rats 11 died without recovering from apnea after trauma, the other 83 animals survived and were examined. All MFP animals demonstrated varying degrees of subarachnoid hemorrhaging, which encompassed the entire brain stem and the basal regions of the cerebral hemispheres (Fig. 1). In the impact site, including the parasagittal cortex of the injured brain, intraparenchymal hemorrhaging was observed as limited foci scattered throughout the corpus callosum and brain stem. Figure 2 shows the time course of the mean TNFα concentrations in the brain tissues before and after impact. The TNFα concentration gradually increased during the first 1 h (25.0 ± 16.2 ng/g brain), rose to the maximal level (43.0 ± 19.0 ng/g brain) at 3 h and then gradually decreased to 34.0 ± 4.0 ng/g brain at 6 h and decreased further to 12.6 ± 13.2 ng/g brain at 24 h.

No visible signal intensities were detected by MRI in the brain pre-impact, but the localized area at the impact site including the corpus callosum and the brain stem showed increased signal intensities 24 h after impact (Fig. 3).

Sham-operated control animals showed no signs of intra-axonal tracer uptake. At 15 min after impact, intra-axonal flooded HRP was observed ultrastructurally in the corpus callosum (Fig. 4) and the brain stem. The frequency of the HRP-flooded axons decreased at 30 min after impact and these were not visualized 1 h after impact.

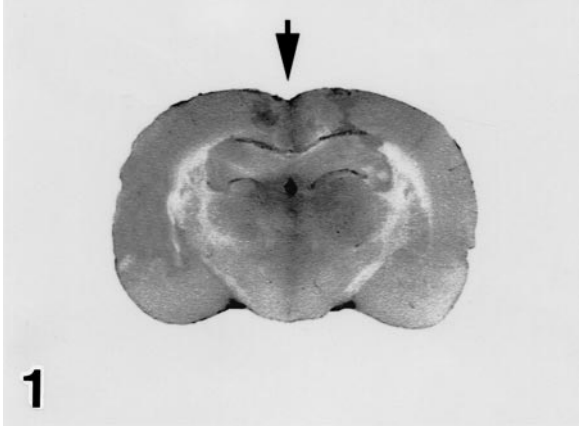

Fig. 1 Midline fluid percussion injury(*arrow*) model rats demonstrated varying degrees of subarachnoid hemorrhage, which encompassed the entire brain stem and the basal regions of the cerebral hemispheres. At the impact site, including the parasagittal cortex of the injured brain intraparenchymal hemorrhaging was observed as limited foci, scattered throughout the corpus callosum and brain stem

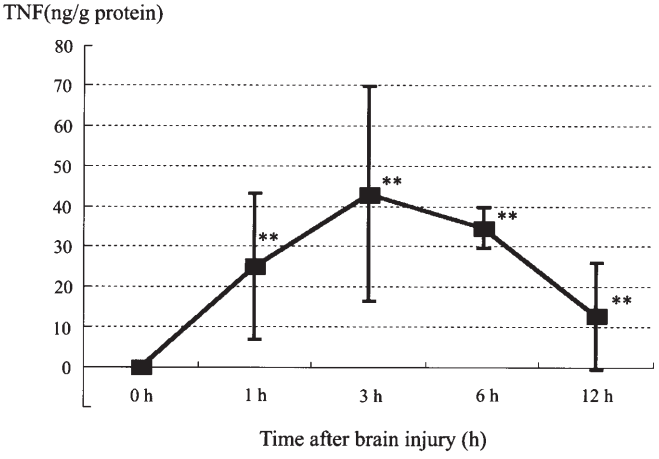

Fig. 2 Mean TNFα concentrations of brain tissue with treatment after impact measured by TNFα ELISA kit. $^{**}p<0.01$ (versus 0 h: pre-impact). Data are expressed as the mean ± SE for five rats

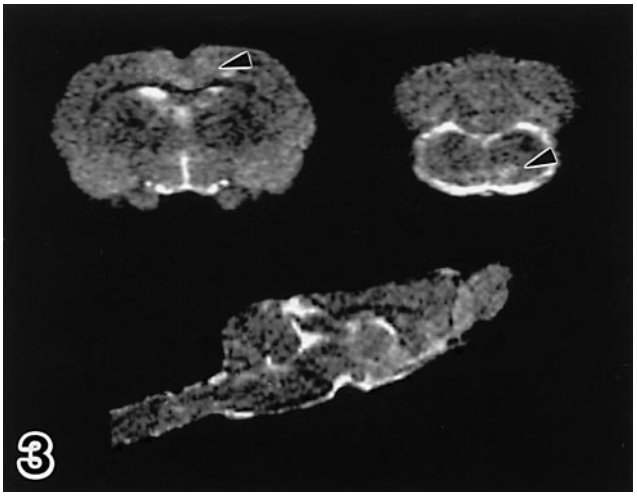

Fig. 3 Coronal T2-weighted image at the level of the anterior hypothalamus at 24 h after impact. The localized area (*arrowheads*) at the impact site including the corpus callosum and the brain stem increased signal intensities

At 1 h after impact, the tracer could be visualized in the periaxonal space in the corpus callosum (Fig. 5) and the brain stem. At 3 h after impact, a few HRP-flooded axons were visualized in the corpus callosum and the brain stem (Fig. 6) and the frequency of the HRP-flooded axons increased from 6 h after impact.

Electron microscopy findings showed that the earliest changes such as the changes noted below in the corpus callosum and the brain stem were noted in axons at 15 min after impact. Elongation of the nodes of Ranvier was frequently observed (Fig. 7) and disruption of the axon was occasionally observed (Fig. 8). Swelling of the mitochondria was also observed at these axons. These disrupted axons decreased with increase in time after impact of less than 1 h. At 1 h post-injury, focal involution of axolemma was observed and microglia accumulated in the corpus callosum (Fig. 9) and the brain stem. These altered axolemma were frequently observed 3 h after impact. At 6 h post-injury, swollen axons with accumulations of organelles were observed in the corpus callosum and the brain stem (Fig. 10) and axonal degeneration, which had a morphology similar to retraction balls at the light microscope level, developed 24 h after impact (Fig. 11). Neutrophils then permeated into the traumatized corpus callosum and brain stem 6 h after impact and disrupted axons were also occasionally observed 24 h after impact (Fig. 12). At 48 h after impact, macrophages were occasionally observed and phagocytosed the disrupted axons (Fig. 13).

By immunoelectron microscopy no immunoreaction of TNFα could be detected in sham-operated control brains, but was occasionally detected in the lysosomes of the microglia (Fig. 14) that had accumulated in the corpus callosum and the brain stem 30 min after impact. At 1 h after impact, lysosomes of glia cells such as microglia, perivascular astrocytes and oligodendroglia were immunoreactive for TNFα at the impact site of the cortex including the corpus callosum and the brain stem. Macrophages (Fig. 15) were occasionally seen in the hemorrhagic con-

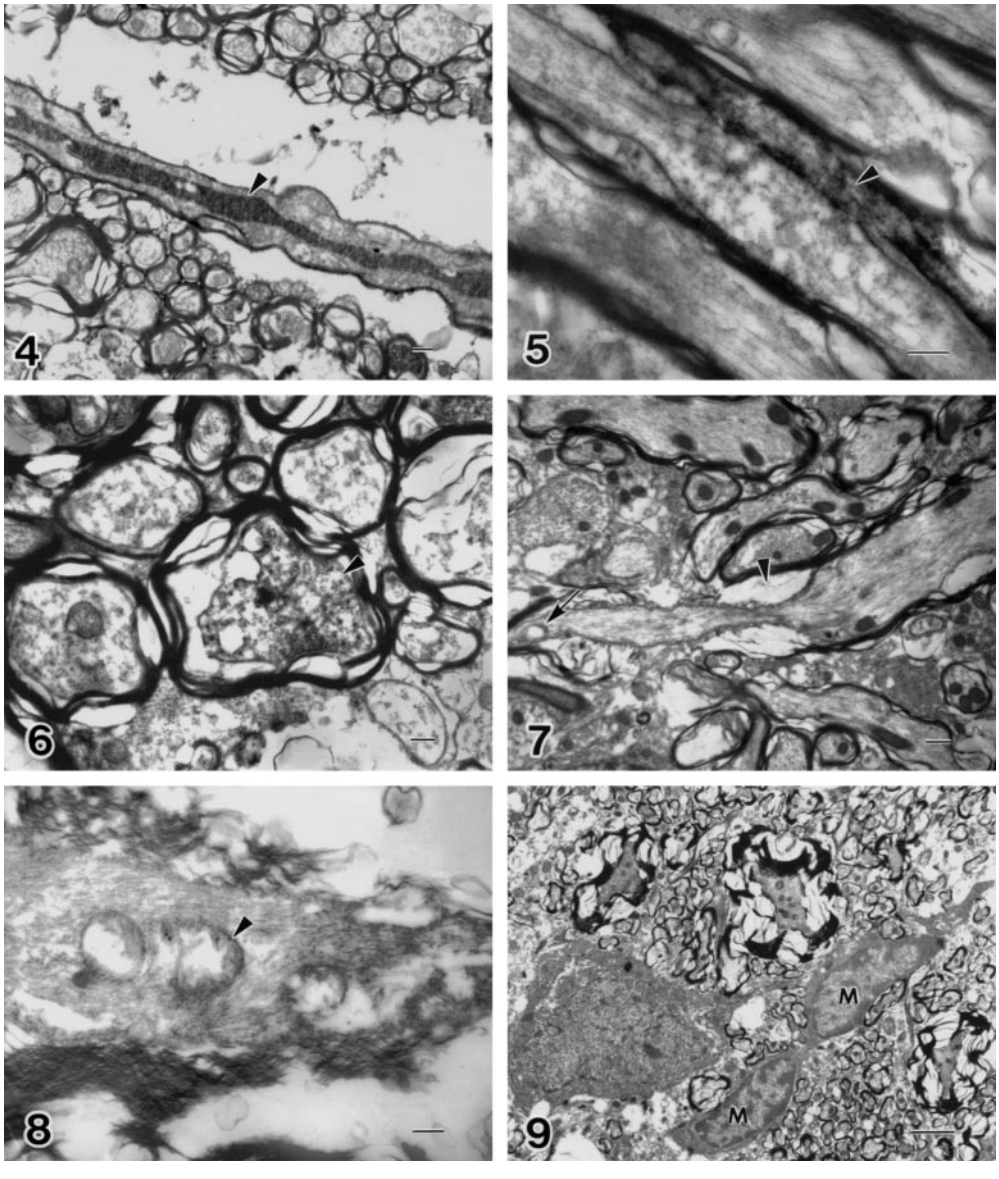

Fig. 4 Electron micrograph of tracer experiments showing the HRP-flooded axons (*arrowhead*) in the corpus callosum 15 min after impact. The frequency of the HRP-flooded axons decreased 30 min after impact and these HRP-flooded axons were not visualized at 1 h after impact. Bar = 500 nm

Fig. 5 Electron micrograph of tracer experiments showing axon in the corpus callosum 1 h after impact. Electron-dense deposits of the tracer (*arrowhead*) exist in the periaxonal space. Bar = 200 nm

Fig. 6 Electron micrograph of tracer experiments showing peroxidase-containing axons (*arrowhead*) in the brain stem 3 h after impact. The frequency of peroxidase-containing axons increased 6 h after impact. Bar = 200 nm

Fig. 7 Electron micrograph showing the node of Ranvier in the corpus callosum 15 min after impact. Elongation of the transverse bands (*arrowhead*) and mitochondrial swelling (*arrow*) were observed. Bar = 500 nm

Fig. 8 Electron micrograph showing the disrupted axon in the corpus callosum 15 min after impact and mitochondrial swelling (*arrowhead*). Bar = 200 nm

Fig. 9 Electron micrograph showing the focal involution axolemma in the corpus callosum 1 h after impact. The microglia cells (*M*) accumulated at these sites. Bar = 2 μm

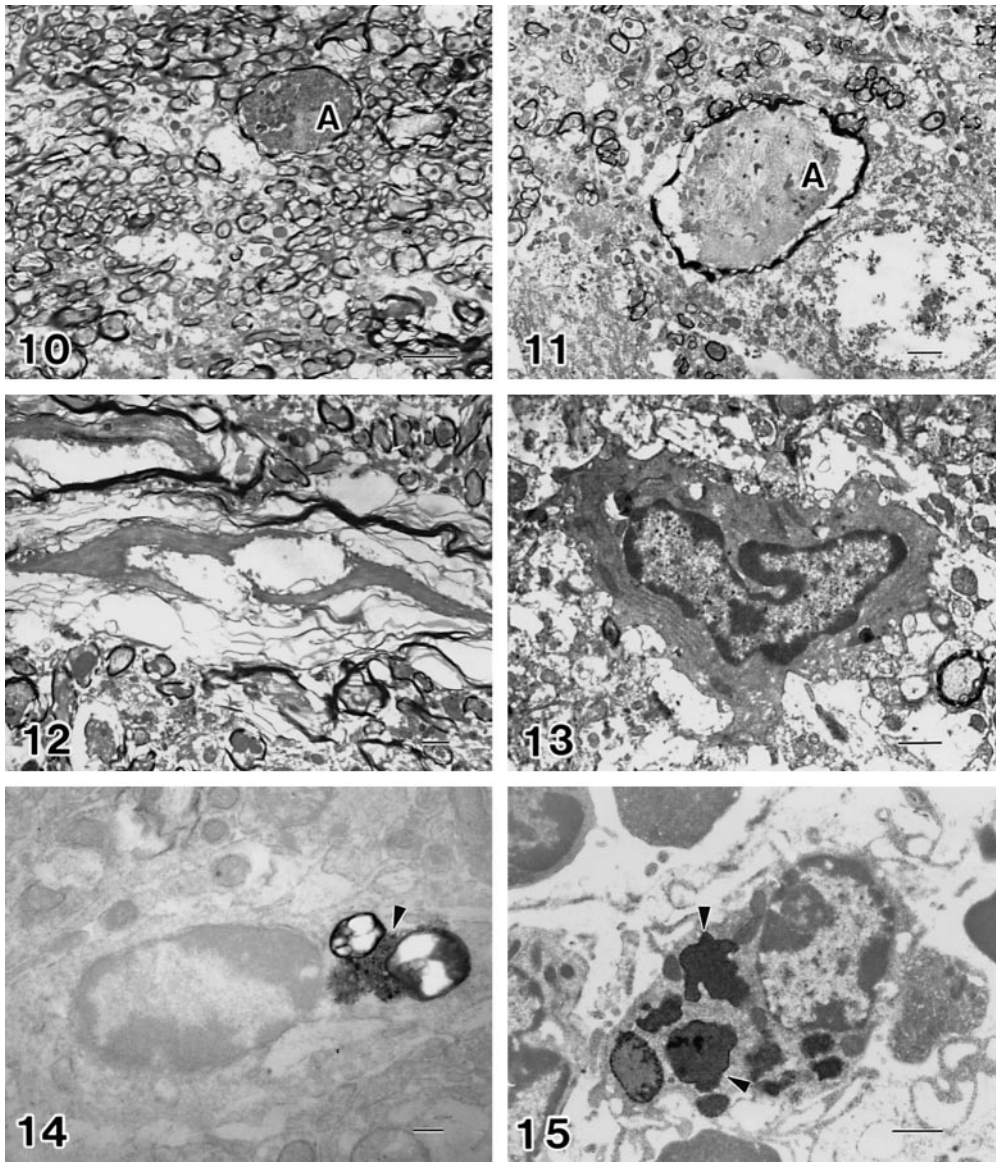

Fig. 10 Electron micrograph showing the swollen axon (*A*) with accumulations of organelles in the brain stem 6 h after impact. Bar = 1 μm

Fig. 11 Electron micrograph showing the swollen axon (*A*) in the corpus callosum 24 h after impact. The axonal degenerations have a morphology similar to retraction balls on the LM levels developed. Bar = 2 μm

Fig. 12 Electron micrograph showing the disrupted axons in the brain stem 24 h after impact. Bar = 1 μm

Fig. 13 Electron micrograph showing a macrophage in the corpus callosum 48 h after impact. Bar = 1 μm

Fig. 14 Electron micrograph showing immunoreactions of TNFα (*arrowhead*) in lysosomes of a microglia in the corpus callosum 30 min after impact. Bar = 200 nm

Fig. 15 Electron micrograph showing immunoreactions of TNFα (*arrowheads*) in lysosomes of a macrophage at the hemorrhagic contusion site of the cortex 1 h after impact. This macrophage in the subarachnoid space may have migrated into the adjacent injured cortex. Bar = 1 μm

tusion site of the cortex and the lysosomes were immunoreactive for TNFα. At 3 h after impact, edematous changes occurred in the oligodendroglia and the vascular feet around the capillaries of the astrocytes at the corpus callosum and the brain stem and the lysosomes of such cells were immunoreactive for TNFα (Fig. 16). This immunoreactivity was more frequently observed 3 and 6 h after impact and persisted for up to 24 h after impact. The appearance of inflammatory cells, with lysosomes immunoreactive for TNFα, frequently increased with the increase in time after impact. There were no immunoreactions of β-APP detected in the sham-operated control brains, but these reactions were detected in the axon of the corpus callosum and brain stem 1 h after impact (Fig. 17) and were more frequently observed 3 and 6 h after impact (Fig. 18).

Discussion

In the present study, MRI investigations showed edematous changes at the impact site including the corpus callosum and the brain stem 24 h after impact. Therefore, our ultrastructural examinations were investigated at the localized areas in the corpus callosum and the brain stem. Electron microscopic investigations revealed axonal retraction balls in the corpus callosum and brain stem from 6 h after impact. Previous DAI experiments using fluid percussion models have indicated that early axonal damage (primary axotomy) is induced by direct head injury and that delayed axonal damage (secondary axotomy) observed in the corpus callosum and brain stem sites may be induced by axolemmal permeability (Pettus et al. 1994; Pettus and Povlishock 1996; Povlishock et al. 1997). These reports also suggested that the occurrence of altered axolemmal permeability and concomitant cytoskeletal

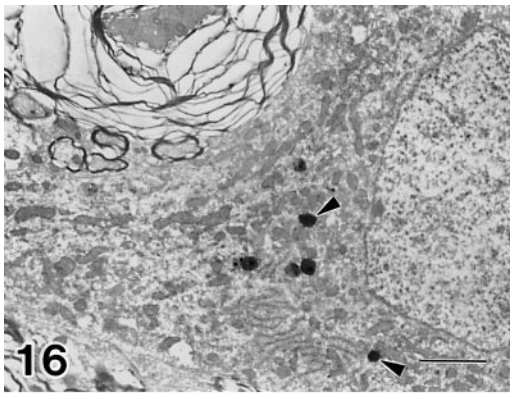

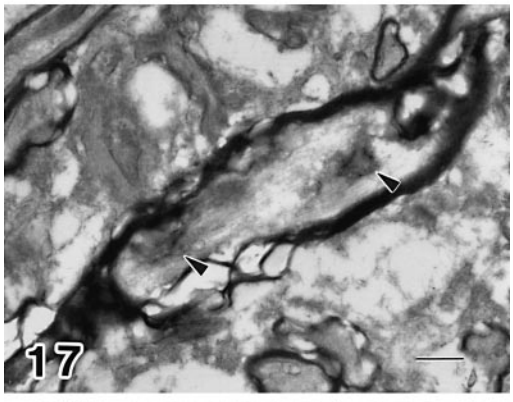

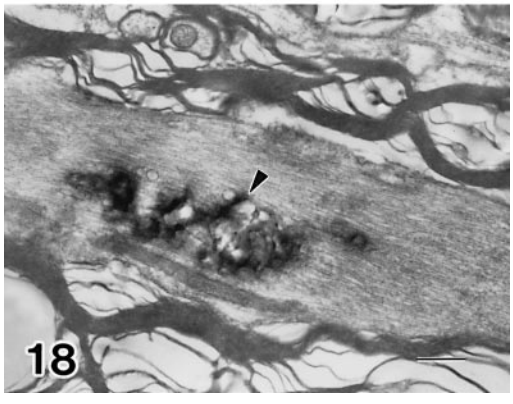

Fig. 16 Electron micrograph showing immunoreactions of TNFα (*arrowheads*) in lysosomes of an oligodendroglia in the brain stem 3 h after impact. Bar = 2 μm

Fig. 17 Electron micrograph showing immunoreactions of β-APP (*arrowheads*) in an axon of the corpus callosum 1 h after impact. Bar = 500 nm

Fig. 18 Electron micrograph showing immunoreactions of β-APP (*arrowhead*) in an axon of the brain stem 3 h after impact corresponding to the axonal vacuole. Bar = 500 nm

changes are features common to traumatic brain injury. Our ultrastructural examinations showed similar results and indicated that primary axotomy can be observed 15 min after impact and delayed secondary axotomy 1 h after impact (Fig. 9). Maxwell et al.(1997) suggested that the occurrence of myelin changes may have been due to a less than adequate fixation rather than reflecting a pathology of the myelin. Therefore, our present DAI experiments were investigated at the time when the external axonal damage, such as alteration of axolemmal permeability, was detected by the tracer experiments which showed that primary axotomy appears as early as 15 min after impact but recovery was immediate. The frequency of the HRP-flooded axons decreased 30 min after impact but were not visualized 1 h after impact. At 1 h after impact, secondary axolemmal permeability increased and the tracers were visualized in the periaxonal space in the corpus callosum and the brain stem. Previous reports indicated that the transverse bands are a means of access to the periaxonal space of the central myelinated nerve fiber and tracers such as peroxidase, invade the periaxonal space through the transverse bands (Hirano and Dembitzer 1969; Feder 1971). Therefore the earliest axonal changes (primary axotomy), such as elongation of the transverse bands, or the disruption of an axon caused the HRP-flooded axons 15 min after impact. Also, secondary alterations of axolemmal permeability may be induced by some delayed endogenous neurotoxic factors. TNFα has been implicated as a major proinflammatory cytokine that is elevated after head injury (Ross et al. 1994; Kita et al. 1997; Feuerstein et al. 1997) and can directly induce primary demyelination and oligodendrocyte apoptosis (Previtali et al. 1997; Akassoglou et al. 1998; Ladiwala et al. 1998). Creange et al. (1997) reviewed that the direct injection of TNFα into nerve induces wallerian degeneration and Madigan et al. (1996) also reported that a dose-dependent axonal loss and degeneration associated with the morphological changes are induced in rabbit optic nerves following intravitreal injection of TNFα indicating that TNFα has a direct myelinotoxic effect. We therefore investigated the immunolocalization of TNFα after traumatic brain injury and investigated the time course of mean TNFα concentrations in the brain tissues before and after impact. Our present TNF assay study demonstrated that TNFα is elevated in brain tissues 1 h after impact. The immunoelectron microscopy study indicated that the immunoreactions of TNFα were detected in microglia as early as 30 min after impact and 1 h after impact were mainly detected in the glial cells such as microglia, perivascular astrocytes and oligodendroglia. Our previous experiment on traumatic head injury using fluid percussion rat models (Kita et al. 1997) demonstrated that microglia are extremely mobile and are easily transported to injured areas within the brain and the present study revealed that microglia are the first cell type to arrive at an injured site. Akassoglou et al.(1998) demonstrated that local production of TNF by the central nervous system glia potently and selectively induced myelin vacuolation and oligodendrocyte apoptosis in the context of the absence of immune cell infiltration. Our previous TNF assay data from the traumatic head injury experiment (Kita et al. 1997) showed that the TNF peak in the cerebrospinal fluid (CSF) was at 6 h, which was perhaps caused by the inflammatory cells, but our present study showed that the peak of TNF concentration in brain tissue is 3 h after impact and that the inflammatory cells appeared 6 h after impact. So the TNF in brain tissue mainly originated from

the glia of the central nervous system. The present study suggests that TNFα contributes to secondary axotomy and this is supported by electron microscopy immunocytochemical evidence of TNF labeling.

Previous studies have demonstrated that the immunocytochemical visualization of β-APP is a useful marker for axonal damage resulting from disruption of the cytoskeleton, leading to abnormalities in the axonal transport of β-APP (McKenzie et al. 1996; Bramlett et al. 1997). Practical and experimental β-APP immunocytochemical data revealed that secondary axonal damage occurs between 1.5 h and 2 h after head injury and the labeling of β-APP is seen to progress with increased survival periods (Blumbergs et al. 1995; McKenzie et al. 1996; Yam et al. 1997; Ogata and Tsuganezawa 1999). The results of our study are similar and immunocytochemical labeling of β-APP was visualized by electron microscopy 1 h after impact. At 3 h after impact, a labeling of β-APP corresponding to the axonal vacuole was observed. The swollen axons, with a focal accumulation of organelles which was observed at 6 h post-injury, may be induced by these abnormalities in axonal transport.

Our present results also showed that external axonal damage reflected by the increase of axolemmal permeability and the internal axonal damage by the abnormality of axonal transport were observed 1 h after impact. Pettus et al. (1994) and Pettus and Povlishock (1996) found that this delayed non-disruptive axonal damage is associated with direct perturbation of the axolemma reflecting its altered permeability. Previous reports have indicated that myelinating glial cells influence the degree of neurofilament phosphorylation and transportation (de-Waegh et al. 1992; Nixon et al. 1994). Therefore, we suggest that the axonal transport abnormality may be caused by the altered axolemmal permeability.

In conclusion, the present study suggests that TNFα conveyed from the glial cells may contribute to the pathogenic mechanism of DAI formation following fluid percussive brain injury.

Acknowledgment This work was supported by a grant-in-aid for scientific research (no. 09670460) from the Ministry of Education of Japan.

References

Akassoglou K, Bauer J, Kassiotis G, Pasparakis M, Lassmann H, Kollias G, Probert L (1998) Oligodendrocyte apoptosis and primary demyelination induced by local TNF/p55TNF receptor signaling in the central nervous system of transgenic mice: models for multiple sclerosis with primary oligodendrogliopathy. Am J Pathol 153:801–813

Blumbergs PC, Scott G, Manavis J, Wainwright H, Simpson DA, McLean AJ (1995) Topography of axonal injury as defined by amyloid precursor protein and the sector scoring method in mild and severe closed head injury. J Neurotrauma 12:565–572

Bramlett HM, Kraydieh S, Green EJ, Dietrich WD (1997) Temporal and regional patterns of axonal damage following traumatic brain injury: a beta-amyloid precursor protein immunocytochemical study in rats. J Neuropathol Exp Neurol 56:1132–1141

Creange A, Barlovatz Meimon G, Gherardi RK (1997) Cytokines and peripheral nerve disorders. Eur Cytokine Netw 8:145–151

de-Waegh SM, Lee VM, Brady ST (1992) Local modulation of neurofilament phosphorylation, axonal caliber, and slow axonal transport by myelinating Schwann cells. Cell 68:451–463

Feder N (1971) Microperoxidase. An ultrastructural tracer of low molecular weight. J Cell Biol 51:339–343

Feuerstein GZ, Wang X, Barone FC (1997) Inflammatory gene expression in cerebral ischemia and trauma. Potential new therapeutic targets. Ann N Y Acad Sci 825:179–193

Geddes JF (1997) What's new in the diagnosis of head injury? J Clin Pathol 50:271–274

Geddes JF, Vowles GH, Beer TW, Ellison DW (1997) The diagnosis of diffuse axonal injury: implications for forensic practice. Neuropathol Appl Neurobiol 23:339–347

Gentleman SM, Roberts GW, Gennarelli TA, Maxwell WL, Adams JH, Kerr S, Graham DI (1995) Axonal injury: a universal consequence of fatal closed head injury? Acta Neuropathol (Berl) 89:537–543

Hirano A, Dembitzer HM (1969) The transverse bands as a means of access to the periaxonal space of the central myelinated nerve fiber. J Ultrastruct Res 28:141–149

Iwamoto Y, Yamaki T, Murakami N, Umeda M, Tanaka C, Higuchi T, Aoki I, Naruse S, Ueda S (1997) Investigation of morphological change of lateral and midline fluid percussion injury in rats, using magnetic resonance imaging. Neurosurgery 40:163–167

Kita T, Liu L, Tanaka N, Kinoshita Y (1997) The expression of tumor necrosis factor-alpha in the rat brain after fluid percussive injury. Int J Legal Med 110:305–311

Ladiwala U, Lachance C, Simoneau SJ, Bhakar A, Barker PA, Antel JP (1998) P75 neurotrophin receptor expression on adult human oligodendrocytes: signaling without cell death in response to NGF. J Neurosci 18:1297–1304

Madigan MC, Rao NS, Tenhula WN, Sadun AA (1996) Preliminary morphometric study of tumor necrosis factor-alpha (TNF alpha)-induced rabbit optic neuropathy. Neurol Res 18:233–236

Matsukawa A, Furukawa S, Ohkawara S, Takagi K, Yoshinaga M (1994) Development of a neutralizing monoclonal antibody against rabbit IL-1 receptor antagonist and utilization for ELISA and measurement of masked IL-1 activity in biological materials. Immunol Invest 23:129–142

Matsukawa A, Fukumoto T, Maeda T, Ohkawara S, Yoshinaga M (1997) Detection and characterization of IL-1 receptor antagonist in tissues from healthy rabbits: IL-1 receptor antagonist is probably involved in health. Cytokine 9:307–315

Maxwell WL, Povlishock JT, Graham DL (1997) A mechanistic analysis of nondisruptive axonal injury: a review. J Neurotrauma 14:419–440

McKenzie KJ, McLellan DR, Gentleman SM, Maxwell WL, Gennarelli TA, Graham DI (1996) Is beta-APP a marker of axonal damage in short-surviving head injury? Acta Neuropathol (Berl) 92:608–613

Merrick BA, He CY, Craig WA, Clark GC, Corsini E, Rosenthal GJ, Mansfield BK, Selkirk JK (1992) Two dimensional gel electrophoresis of cellular and secreted proteins from rat alveolar macrophages after lipopolysaccharide treatment. Appl Theor Electrophor 2:177–187

Nixon RA, Paskevich PA, Sihag RK, Thayer CY (1994) Phosphorylation on carboxyl terminus domains of neurofilament proteins in retinal ganglion cell neurons in vivo: influences on regional neurofilament accumulation, interneurofilament spacing, and axon caliber. J Cell Biol 126:1031–1046

Ogata M, Tsuganezawa O (1999) Neuron-specific enolase as an effective immunohistochemical marker for injured axons after fatal brain injury. Int J Legal Med 113:19–25

Ozawa Y, Nakamura T, Sunami K, Kubota M, Ito C, Murai H, Yamaura A, Makino H (1991) Study of regional cerebral blood flow in experimental head injury: changes following cerebral contusion and during spreading depression. Neurol Med Chir (Tokyo) 31:685–690

Pettus EH, Povlishock JT (1996) Characterization of a distinct set of intra-axonal ultrastructural changes associated with traumatically induced alteration in axolemmal permeability. Brain Res 722 : 1–11

Pettus EH, Christman CW, Giebel ML, Povlishock JT (1994) Traumatically induced altered membrane permeability: its relationship to traumatically induced reactive axonal change. J Neurotrauma 11 : 507–522

Povlishock JT (1992) Traumatically induced axonal injury: pathogenesis and pathobiological implications. Brain Pathol 2 : 1–12

Povlishock JT, Marmarou A, McIntosh T, Trojanowski JQ, Moroi J (1997) Impact acceleration injury in the rat: evidence for focal axolemmal change and related neurofilament sidearm alteration. J Neuropathol Exp Neurol 56 : 347–359

Previtali SC, Archelos JJ, Hartung HP (1997) Modulation of the expression of integrins on glial cells during experimental autoimmune encephalomyelitis. A central role for TNF-alpha. Am J Pathol 151 : 1425–1435

Ross SA, Halliday MI, Campbell GC, Byrnes DP, Rowlands BJ (1994) The presence of tumour necrosis factor in CSF and plasma after severe head injury. Br J Neurosurg 8 : 419–425

Yam PS, Takasago T, Dewar D, Graham DI, McCulloch J (1997) Amyloid precursor protein accumulates in white matter at the margin of a focal ischaemic lesion. Brain Res 760 : 150–157

Yamaki T, Murakami N, Iwamoto Y, Yoshino E, Nakagawa Y, Ueda S, Horikawa J, Tsujii T (1994) A modified fluid percussion device. J Neurotrauma 11 : 613–622